

HETEROCYCLES, Vol. 89, No. 4, 2014, pp. 971 - 980. © 2014 The Japan Institute of Heterocyclic Chemistry
Received, 14th December, 2014, Accepted, 26th February, 2014, Published online, 13th March, 2014
DOI: 10.3987/COM-13-12915

SYNTHESIS AND PHOTOPHYSICAL PROPERTIES OF NEW PYRAZOLINO[60]FULLERENES WITH FLUORENYL AND FLUORINATED PHENYL SUBSTITUENTS

Subo Shen,^a Shanshan He,^a Haonan Cheng,^a Changrui Xu,^a Hongmei Deng,^a
and Jianmin Zhang^{a,b*}

^aDepartment of Chemistry, College of Sciences, Shanghai University 200444, No. 99, Shangda road, Shanghai, P. R. China. ^bKey Laboratory of Organofluorine Chemistry, Shanghai Institute of Organic Chemistry 200032, Chinese Academy of Sciences, No. 354, Fenglin road, Shanghai, P. R. China
E-mail: bobobao1989@shu.edu.cn; jmzhang@shu.edu.cn

Abstract – Two types of triads based on pyrazolino[60]fullerenes with fluorenyl and fluorinated phenyl substituents have been synthesized via the [3+2] dipolar cycloaddition reaction between C₆₀ and corresponding hydrazones in good yields. Photophysical properties of these triads have also been systematically investigated, and their weak emissions indicated fluorescent quenching induced by intramolecular charge transfer may occur between the donor and acceptor parts of these systems.

INTRODUCTION

Since the disclosure of novel and unique electronic properties of fullerene in the past decades, it has become a burgeoning interest in the areas of organic photovoltaics,^{1-3,7} traditional organic synthesis,⁴⁻⁶ and nanotechnology.^{8,9} In recent years, the application of C₆₀ fullerene derivatives^{10,11} in the field of optoelectronic devices has received great attention,¹²⁻¹⁷ and there is an urgent need to improve and optimize the synthetic methods of optoelectronic active C₆₀ fullerene derivatives.

Our previous works have shown the efficient synthesis of fluorophore substituted pyrazolino[60]fullerene derivatives,^{18,19} and these studies were limited to single type of heterocyclic products, we are anxious to make innovation on the design of the product structures. Considering about good fluorescence properties of fluorene derivatives and special electronic effect of fluorine benzene, we decided to introduce fluorene and fluorinated phenyl to fullerene C₆₀. Our continued interest promotes us to extend our research to multiple substituted pyrazolino[60]fullerene derivatives by using asymmetric 1,3-dipole hydrazones.

Based on the symmetrical models (shown in **Figure 1**) we have designed two types of pyrazolino[60]fullerenes triads with fluorenyl and fluorinated phenyl substituents. Based on a large number of related literatures, such a design concept on the applications of fullerenes is not very common. Herein, we present optimized synthesis of these compounds and the detailed investigations of their photophysical properties by UV-VIS absorption and fluorescence spectra.

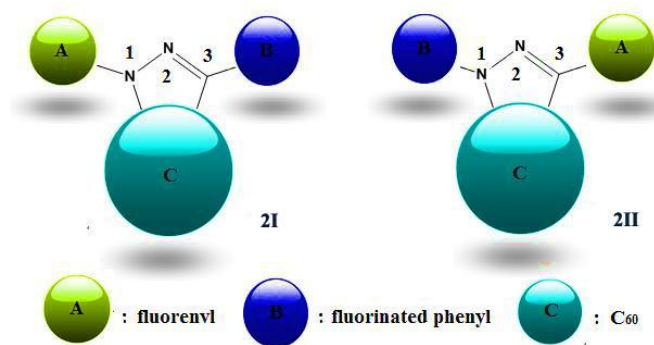
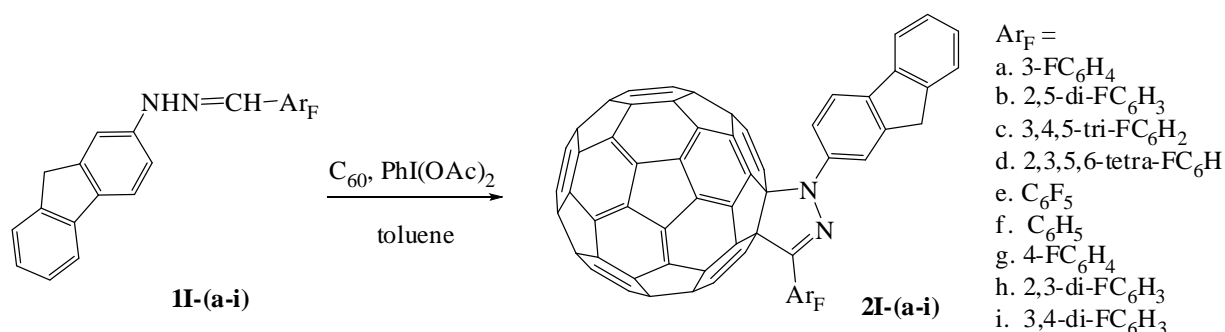


Figure 1. The symmetrical models used in the design of pyrazolino[60]fullerene derivatives

RESULTS AND DISCUSSION

Fluorenyl and fluorinated phenyl groups were chosen as fluorophores A and B. Type I and Type II products were obtained by treating the hydrazone intermediates with fullerene (**Schemes 1 and 2**). In view of our previous research on synthesis of pyrazoline derivatives,¹⁹ a series of hydrazones **1I-(a-i)** were prepared in our general works for another publication, and they were introduced to C₆₀ via the [3+2] dipolar cycloaddition reaction.²⁰⁻²² The synthetic route of target compounds **2I-(a-i)** is shown in **Scheme 1**.



Scheme 1. The synthetic route of **2I-(a-i)**

The reaction of hydrazones **1I-a** with C₆₀ in the presence of PhI(OAc)₂ was chosen as the model reaction to screen the optimized conditions. The screening results of the optimized conditions are summarized in **Table 1**.

It was found that the yield of the product **2I-a** could be improved by increasing the reaction time (entries 1~3). However, the excessive extension of time had a negligible effect on the product yield. Changing the ratio of reactants could also affect the yield of product **2I-a** (entries 2, 4, 5). In addition, an adverse effect was observed on the yields of products by raising the reaction temperature due to the appearance of a large number of impurities (entries 2, 6, 7). Using other solvents, such as benzene or chlorobenzene could not improve the reaction yield (entry 8). After careful comparisons, the best reaction condition was selected as C₆₀ (0.1 mmol), **1I** (0.2 mmol) and PhI(OAc)₂ (0.2 mmol) in 40 mL of toluene at 30 °C for 5 h (entry 2).

Table 1. Optimization of the reaction conditions in one-pot 1,3-dipolar cycloadditions between C₆₀ and hydrazone **1I-a**

Entry	Mole ratio ^a	Solvent	Temperature (°C)	Time (h)	Yield ^b (%) of 2I-a
1	2:2:1	toluene	30	3	16 (75)
2	2:2:1	toluene	30	5	34 (74)
3	2:2:1	toluene	30	7	35 (72)
4	1:1:1	toluene	30	5	17 (70)
5	4:4:1	toluene	30	5	36 (75)
6	2:2:1	toluene	20	5	28 (70)
7	2:2:1	toluene	45	5	30 (67)
8	2:2:1	benzene	30	5	32 (70)

^a Molar ratio refers to **1I-a** : PhI(OAc)₂ : C₆₀. ^b Yields out of parentheses are isolated yields. Yields in parentheses are conversion yields based on reacted C₆₀.

According to the optimized reaction conditions, a series of target compounds **2I-(a-i)** have been prepared. As shown in **Table 2**, all products of Type I afforded 32-37% isolated yields (70–76% yields based on reacted C₆₀).

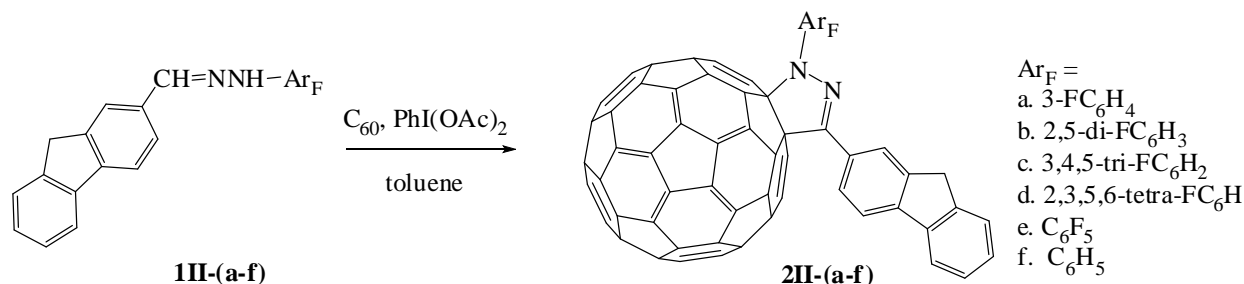
Table 2. Preparation of a series of Type I products **2I-(a-i)**

Entry	Ar _F of reactants 1I-(a-i)	Product 2I-(a-i) ^a	Yield ^b (%)
1	3-FC ₆ H ₄	2I-a	34 (74)
2	2,5-di-FC ₆ H ₃	2I-b	34 (73)
3	3,4,5-tri-FC ₆ H ₂	2I-c	33 (72)
4	2,3,5,6-tetra-FC ₆ H	2I-d	35 (75)
5	C ₆ F ₅	2I-e	37 (76)
6	C ₆ H ₅	2I-f	32 (71)
7	4-FC ₆ H ₄	2I-g	33 (75)
8	2,3-di-FC ₆ H ₃	2I-h	33 (70)
9	3,4-di-FC ₆ H ₃	2I-i	32 (74)

All reactions were performed in toluene at 30 °C for 5 h. ^a Mole ratio refers to **1I-(a-i)** : PhI(OAc)₂ : C₆₀ = 2:2:1; ^b Yields out of parentheses are isolated yields. Yields in parentheses are conversion yields based on reacted C₆₀.

The other type of target compounds **2II-(a-f)** has also been prepared in a similar manner, which is shown in **Scheme 2**.

Similar screening processes of the optimized reaction conditions between C_{60} and **1II-a** are shown in **Table 3**.



Scheme 2. One-pot preparation of **2II-(a-f)**

Table 3. Optimization of the reaction conditions in one-pot 1,3-dipolar cycloaddition between C_{60} and hydrazone **1II-a**

Entry	Mole ratio ^a	Solvent	Temperature (°C)	Time (h)	Yield ^b (%) of 2II-a
1	2:2:1	toluene	40	3	20 (71)
2	2:2:1	toluene	40	5	34 (72)
3	2:2:1	toluene	40	7	34 (69)
4	1:1:1	toluene	40	5	16 (73)
5	4:4:1	toluene	40	5	35 (71)
6	2:2:1	toluene	30	5	30 (74)
7	2:2:1	toluene	60	5	25 (63)
8	2:2:1	benzene	40	5	32 (70)

^a Molar ratio refers to **1II-a** : PhI(OAc)₂ : C_{60} . ^b Yields out of parentheses are isolated yields. Yields in parentheses are conversion yields based on reacted C_{60} .

According to the optimized reaction conditions, a series of target compounds **2II-(a-f)** have been prepared. As shown in **Table 4**, all the products of Type II afforded 33-38% isolated yields (70–79% yields based on reacted C_{60}).

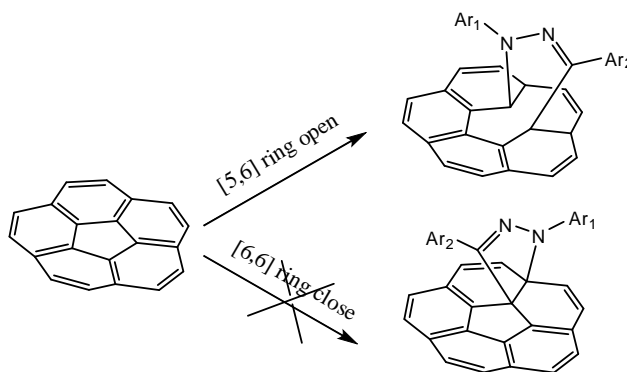
Table 4. Preparation of a series of Type II products **2II-(a-f)**

Entry	Ar _F of reactants 1II-(a-f)	Product 2II-(a-f) ^a	Yield ^b (%)
1	3-FC ₆ H ₄	2II-a	34 (72)
2	2,5-di-FC ₆ H ₃	2II-b	33 (70)
3	3,4,5-tri-FC ₆ H ₂	2II-c	35 (70)
4	2,3,5,6-tetra-FC ₆ H	2II-d	35 (75)
5	C ₆ F ₅	2II-e	38 (79)
6	C ₆ H ₅	2II-f	33 (70)

All reactions were performed in toluene at 30 °C for 5 h. ^a Mole ratio refers to **1II-(a-f)** : PhI(OAc)₂ : C₆₀ = 2:2:1; ^b Yields out of parentheses are isolated yields. Yields in parentheses are conversion yields based on reacted C₆₀.

It's worth mentioning that the yields of the products **2I** and **2II** are very close to each other regardless of the number or the substitution position of fluorine atoms on the benzene ring. Generally, the reaction yield would be reduced by the influence of electron-withdrawing group, but the expected results were not observed. This phenomenon may be caused by the increasing of the reactants solubility in the solvent by the introduction of fluorine atoms.

The structures of all products **2I** and **2II** were fully characterized by spectroscopic methods (UV-VIS, FTIR, ¹H NMR, ¹⁹F NMR, ¹³C NMR, and MALDI-FTICR-MS). The mass spectra of the products **2I** and **2II** exhibit the expected [M]⁺ or [M+H]⁺ peaks and well matching the calculated molecular weights. The ¹H and ¹⁹F NMR spectra display the expected chemical shifts and splitting patterns for all protons and fluorine atoms. For instance, in the ¹³C NMR spectra of **2I-f**, 48 peaks appear in the range of 119-148 ppm, and among them 4 peaks are due to the sp² carbons of benzene ring, 12 peaks are due to the sp² carbons of fluorenyl moiety and other 32 peaks are caused by C₆₀ skeleton. It is indicated that the pyrazolelin ring is formed between a pentatomic ring and a hexatomic ring to get the [5,6] ring open products (**Scheme 3**). Two peaks at about 92.23 and 81.46 ppm are assigned to the two sp³ carbons of C₆₀, and the peak at 37.11 ppm is related to the sp³ carbon of the fluorenyl moiety.

**Scheme 3.** The products are [5,6] ring open but not [6,6] ring close

UV-VIS absorption and fluorescence spectra for comparison in symmetrical types

After testing different concentrations of the products, 6×10^{-6} mol/L in CHCl_3 was chosen as the best condition for the ultraviolet analysis of **1I-(a-e)**, **1II-(a-e)**, **2I-(a-e)** and **2II-(a-e)**. As shown in **Figure 2**, **2I-(a-e)** show stronger ultraviolet absorption due to the expansion of better electron transportation after C_{60} connecting with **1I-(a-e)**, this rule also applies to Type II. Considering about the peak positions, the peaks of **1I-(a-e)** and **1II-(a-e)** in 250~270 nm are due to $\pi-\pi^*$ electronic transitions, and peaks in 300~350 nm are caused by fluorenyl moiety. The peaks of **2I-(a-e)** and **2II-(a-e)** in 280~330 nm are caused by fluorenyl moiety, peaks in 250~260 nm are caused by C_{60} .

1II-(a-e) show two absorption bands centered at 250 and 325 nm respectively, which could be attributed to the $\pi-\pi^*$ transition and intramolecular charge transfer process between fluorenyl (donor) and fluorinated substituents (acceptor). However, in the spectra of **1I-(a-e)**, only tiny peaks in the latter bands could be observed. The lack of charge transfer bands indicate the intramolecular charge transfer process may largely be prohibited in the **1I-(a-e)** series. This difference may arise from the better electron transportation of fluorenyl and fluorinated groups in the structure of the **1II-(a-e)** series. This difference was not observed in the UV-vis spectra of **2I-(a-e)** and **2II-(a-e)**, and all of them show the characteristic absorption bands of the $\pi-\pi^*$ transition and intramolecular charge transfer process. This may indicate that the fullerene part as an acceptor takes part in the intramolecular charge transfer process in the triads system, and this transfer pathway may be superior than the way through fluorenyl and fluorinated groups.

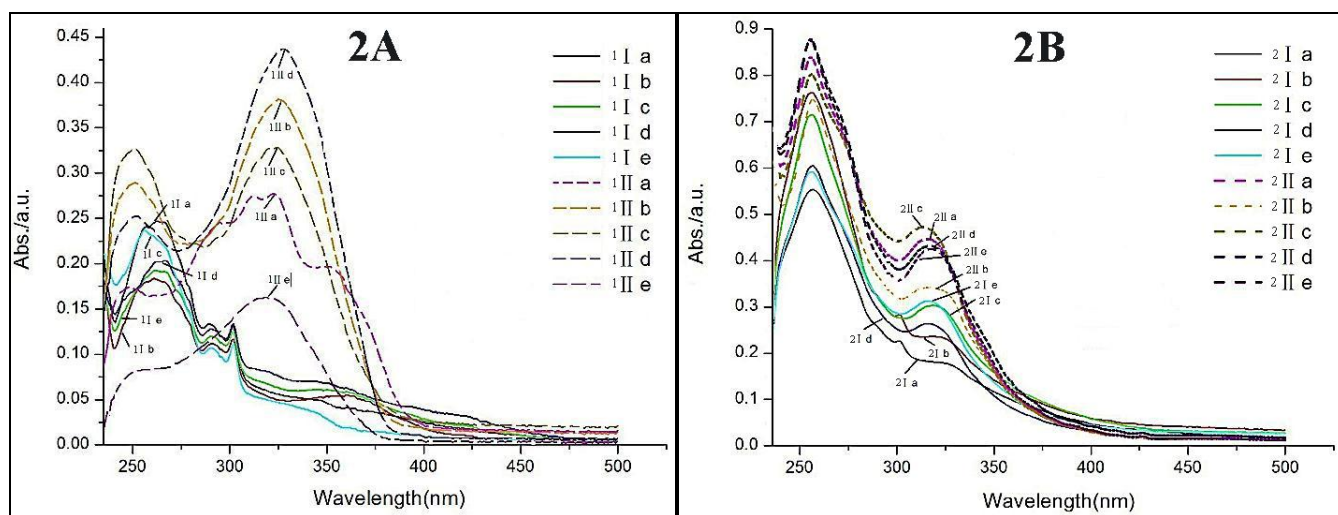


Figure 2. UV spectra of compounds **1I**, **1II** (**2A**) and **2I**, **2II** (**2B**) in CHCl_3 at room temperature

First of all, the fluorescence intensities of **1I-(a-e)** are stronger than **1II-(a-e)** as shown in **Figure 3**. The fluorescence intensities of **1II-(a-e)** decrease along with the increasing of fluorine atom number on the phenyl. Second, it was found that products **2I-(a-e)** and **2II-(a-e)** both display weaker fluorescence intensity than reactants obviously which is caused by fluorescence quenching of the compounds with C_{60} .

The fluorescence spectra of **2I-(a-e)** and **2II-(a-e)** tend to be similar—two main absorption peaks appear at about 412 and 440 nm. The fluorescence intensities decrease obviously when the hydrazone derivatives **1I-(a-e)** and **1III-(a-e)** synthesized to be the pyrazolino C₆₀ derivatives. We inferred that the too-strong electron-withdrawing effect of C₆₀ changes the electron transferring in pyrazolino C₆₀ derivatives, and this effect makes the fluorescence properties of **2I-(a-e)** and **2II-(a-e)** to be similar.

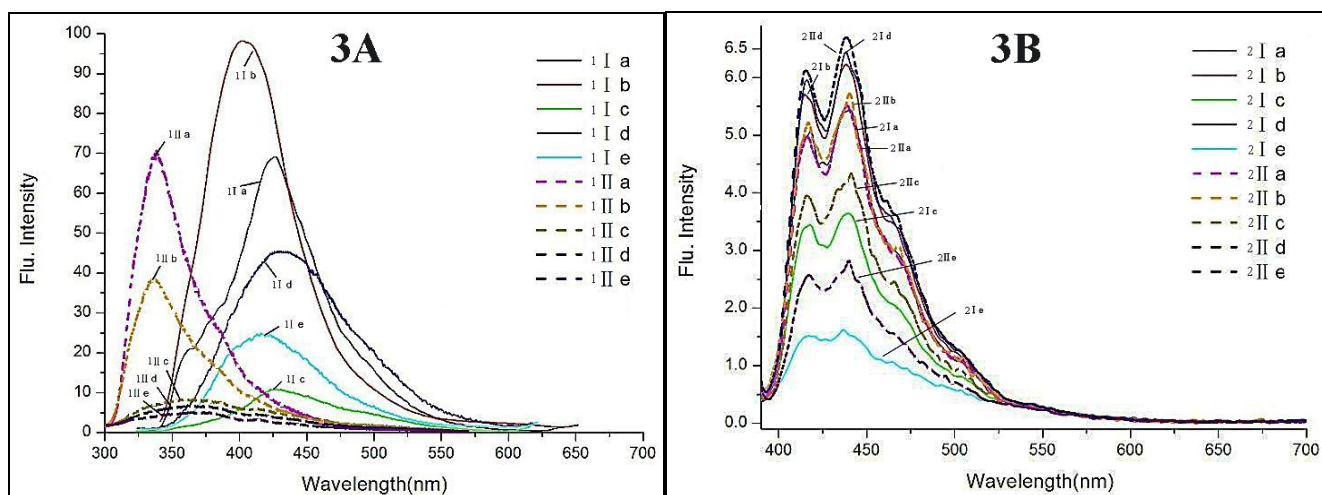


Figure 3. Fluorescence spectra of **1I**, **1III** (**3A**) and **2I**, **2II** (**3B**) in CHCl₃ at room temperature

Electrochemical examinations

In order to further verify electronic transmission of Type I and Type II products, some of them were chosen to be tested by CV(cyclic voltammetry). In **Figure 4**, products **2I-a** and **2II-a** show a quasi-reversible electrochemical behavior, product **2I-a** has two one-electron reduction waves at -1.91V and -1.27V. However, product **2II-a** shows three one-electron reduction waves at -1.96V, -1.54V and -0.93V. Furthermore, the products of Type I show similar shape to **2I-a**, which is also applied to Type II.

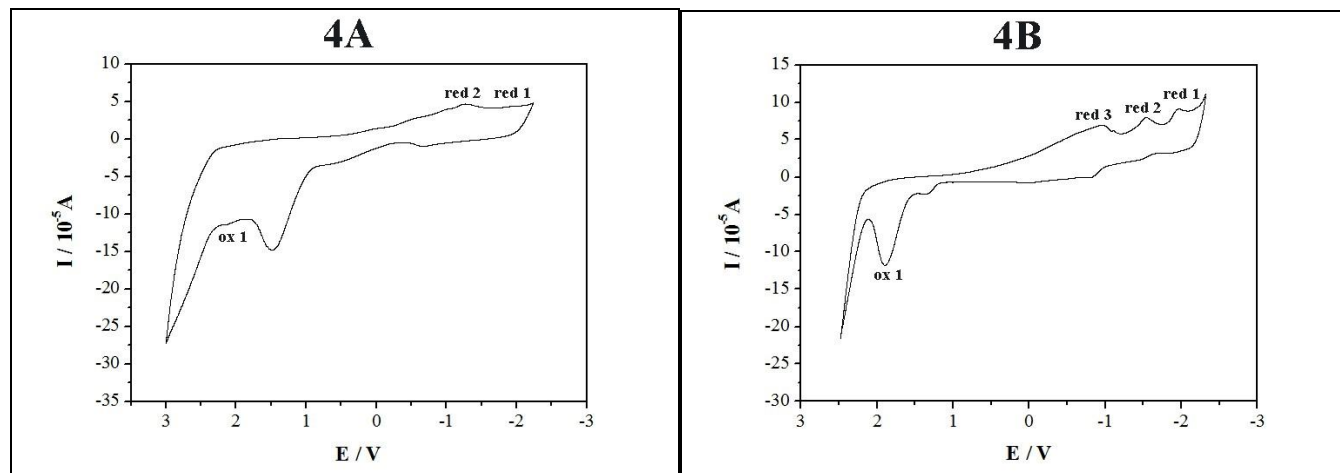


Figure 4. Cyclic voltammogram of products **2I-a** (**4A**) and **2II-a** (**4B**)

All the initial reduction of voltages vs Fc/Fc⁺ were used to calculate LUMO energies of the products. If the initial oxidation voltages were chosen to calculate HOMO energies, values of HOMO energies and LUMO-HOMO energy gaps (E_g) would be get out of parentheses in **Table 5**. On the other hand, combined with the edge of the UV peak wavelength, LUMO-HOMO energy gaps (E_g) could be obtained approximately in parentheses, then HOMO energies could also been calculated by LUMO energies and LUMO-HOMO energy gaps. After data analysis, it was found that the results obtained by the two different calculation methods are relatively uniform. The most important point should be emphasized that LUMO-HOMO energy gaps (E_g) of Type II products are about 0.1~0.3 eV smaller than that of Type I products, enabling an easier electron-transfer process.

Table 5. The LUMO and HOMO energies and LUMO-HOMO energy gaps (E_g) were calculated

Compound	E _{red 1} (V)	E _{red 2} (V)	E _{red 3} (V)	E _{ox 1} (V)	E _{red} ^a (V)	LUMO (eV)	HOMO ^b (eV)	E _g ^b (eV)
C ₆₀ [23]	—	—	—	—	—	-3.22	-5.98	2.76
2I-a	-1.91	-1.27	—	2.14	-1.18	-3.62	-7.67(7.26)	4.05(3.64)
2I-d	-2.04	-1.54	-1.09	1.89	-1.31	-3.49	-7.42(6.89)	3.93(3.40)
2I-h	-2.04	-1.54	-0.86	1.88	-1.31	-3.49	-7.41(6.91)	3.92(3.42)
2I-i	-1.99	-1.54	-1.09	1.83	-1.26	-3.54	-7.36(6.89)	3.82(3.35)
2II-a	-1.96	-1.54	-0.93	1.88	-1.23	-3.57	-7.41(6.88)	3.84(3.31)
2II-c	-1.99	-1.55	-1.10	1.90	-1.26	-3.54	-7.43(6.80)	3.89(3.26)
2II-d	-2.02	-1.53	-1.03	1.87	-1.29	-3.51	-7.40(6.76)	3.89(3.25)

^a E_{red} is the first half-wave reduction potential of the compound relative to Fc/Fc⁺. ^b Values out of parentheses are calculated by initial oxidation voltages. Values in parentheses are calculated by the edge of the UV peak wavelength.

In summary, two types of asymmetric pyrazolino[60]fullerenes derivatives with various fluorenyl and fluorinated substituents have been synthesized via the [3+2] dipolar cycloaddition reaction between C₆₀ and corresponding hydrazones. By this method, we have successfully introduced fluorescent fluorenyl groups onto C₆₀ backbones, and it offers an effective way to synthesize asymmetric pyrazolino[60]fullerenes with different substituents. The investigation of UV-VIS absorption and fluorescence spectra indicated that the existence of effective intramolecular charge transfer process between fluorenyl and fluorinated substituents in the **1I** and **1II** series, and this process could be perturbed by the intramolecular charge transfer process between fluorenyl groups and fullerene in **2I** and **2II** series. Further studies on the synthesis of other fluorophores substituted pyrazolino[60]fullerenes, and detailed investigation of the intramolecular charge transfer process in our systems are ongoing.

EXPERIMENTAL

Typical procedure for the synthesis of 1-(*N*-fluorenyl)-3-(3'-fluorophenyl)pyrazolino[C₆₀]fullerene (2I-a). A mixture of C₆₀ (72 mg, 0.1 mmol), hydrazone 1I-a (60.4 mg, 0.2 mmol) and PhI(OAc)₂ (64 mg, 0.2 mmol) were dissolved in 40 mL of toluene and stirred at 30 °C for 5 h. The solvent was then evaporated in vacuum and the residue was separated on a silica gel column using CS₂ or CS₂-toluene as the eluent to afford unreacted C₆₀ and the adduct 2I-a; Brown solid; IR (KBr, cm⁻¹): ν 3455, 2919, 2850, 1605, 1578, 1047, 574, 526; ¹H NMR (500 MHz, CS₂-CDCl₃): δ 8.32–8.29 (m, 2H), 8.06 (s, 1H), 7.95 (d, *J* = 8.0 Hz, 1H), 7.81 (d, *J* = 8.0 Hz, 1H), 7.74 (d, *J* = 7.5 Hz, 1H), 7.52 (d, *J* = 7.5 Hz, 1H), 7.36 (t, *J* = 7.5 Hz, 1H), 7.28 (t, *J* = 7.5 Hz, 1H), 7.21 (t, *J* = 8.5 Hz, 2H), 3.98 (s, 2H); ¹⁹F NMR (470 MHz, CS₂-CDCl₃): δ -109.02 (s, 1F); ¹³C NMR (125 MHz, CS₂-CDCl₃): δ 162.50, (d, *J* = 246.25 Hz), 147.23, 146.85, 146.03, 145.92, 145.64, 145.59, 145.53, 145.46, 145.43, 145.14, 144.90, 144.82, 144.80, 144.17, 143.94, 143.93, 143.08, 142.83, 142.81, 142.59, 142.53, 142.12, 142.06, 141.93, 141.84, 141.58, 141.41 (d, *J* = 2.5 Hz); 140.83, 139.99, 139.47, 139.06, 137.17, 136.21, 135.95, 134.45 (d, *J* = 8.75 Hz), 130.01 (d, *J* = 8.75 Hz), 128.74, 128.00, 126.76, 126.50, 125.11, 124.79, 123.93, 123.90, 122.97, 120.78, 120.03, 119.63, 115.82 (d, *J* = 21.25 Hz), 115.44 (d, *J* = 22.5 Hz), 92.30 (sp³ C of C₆₀ sphere), 80.83 (sp³ C of C₆₀ sphere), 37.05; MALDI-FTICR-MS: [M]⁺ Calculated for C₈₀H₁₃N₂F₁: 1020.1073; found 1020.10573.

Electrochemical measurements were performed using a Base 2000 CV system electrochemical analyzer. Cyclic voltammetric measurements were carried out in *o*-dichlorobenzene/acetonitrile (4:1) containing 0.1 M *n*-Bu₄NPF₆ as a supporting electrolyte, using a Pt working electrode (φ=1 mm) with ferrocene, and a vitreous carbon rod counter electrode, scan rate: 100 mV/s.

ACKNOWLEDGEMENTS

This work was supported by the National Natural Science Foundation of China (Nos. 21272151). The authors thank the Instrumental Analysis & Research Center of Shanghai University and Doctor Deng, Hongmei.

REFERENCES

1. I. S. Doe, J. Smith, and P. Roe, *J. Am. Chem. Soc.*, 1968, **90**, 8234.
2. Y. Y. Liang, Z. Xu, J. B. Xia, S. T. Tsai, Y. Wu, G. Li, C. Ray, and L. P. Yu, *Adv. Mater.*, 2010, **22**, 135.
3. H. Y. Chen, J. Hou, S. Zhang, Y. Liang, G. Yang, Y. Yang, L. Yu, Y. Wu, and G. Li, *Nat. Photonics*, 2009, **3**, 649.
4. R. Lydia, J. L. Sabina, R. D. Luis, A. J. John, and R. Ponnadurai, *Heterocycles*, 2012, **84**, 719.
5. C. B. Miao, Z. Y. Tian, X. J. Ruan, X. Q. Sun, and H. T. Yang, *Heterocycles*, 2011, **83**, 1615.

6. K. Tsubaki, Y. Murata, K. Komatsu, T. Kinoshita, and K. Fuji, [*Heterocycles*, 1999, **51**, 2553.](#)
7. C. J. Brabec, N. S. Sariciftci, and J. C. Hummelen, [*Adv. Funct. Mater.*, 2001, **11**, 15.](#)
8. D. Gust, T. A. Moore, and A. L. Moore, [*Acc. Chem. Res.*, 2001, **34**, 40.](#)
9. H. B. Liu, J. L. Xu, Y. J. Li, and Y. L. Li, [*Acc. Chem. Res.*, 2010, **43**, 1496.](#)
10. S. S. Babu, H. Mohwald, and T. Nakanishi, [*Chem. Soc. Rev.*, 2010, **39**, 4021.](#)
11. J. L. Delgado, N. Martin, P. Cruz, and F. Langa, [*Chem. Soc. Rev.*, 2011, **40**, 5232.](#)
12. H. Y. Zhao, Z. B. Liu, X. L. Zhang, and J. G. Tian, [*Chin. J. Chem.*, 2012, **30**, 1766.](#)
13. T. Bura, N. Leclerc, S. Fall, P. Leveque, and T. Heiser, [*J. Am. Chem. Soc.*, 2012, **134**, 17404.](#)
14. C. D. Guo, W. R. Teng, H. X. Wu, J. Z. Shen, and X. M. Deng, [*Chin. J. Chem.*, 2005, **23**, 1113.](#)
15. T. Michinobu, K. Okoshi, Y. Murakami, K. Shigehara, K. Ariga, and T. Nakanishi, [*Langmuir*, 2013, **29**, 5337.](#)
16. D. Peckus, A. Devizis, R. Augulis, S. Graf, D. Hertel, and V. Gulbinas, [*J. Phys. Chem. C.*, 2013, **117**, 6039.](#)
17. J. D. Wood, J. L. Jellison, A. D. Finke, and L. C. Wang, [*J. Am. Chem. Soc.*, 2012, **134**, 15783.](#)
18. B. Q. Lu, J. M. Zhang, and J. Li, [*Tetrahedron*, 2012, **68**, 8924.](#)
19. B. Q. Lu, J. M. Zhang, and M. J. Wang, [*Chin. J. Chem.*, 2012, **30**, 1345.](#)
20. H. T. Yang, X. J. Ruan, C. B. Miao, and X. Q. Sun, [*Tetrahedron Lett.*, 2010, **51**, 6056.](#)
21. Y. Matsubara, H. Tada, S. Nagase, and Z. I. Yoshida, [*J. Org. Chem.*, 1995, **60**, 5372.](#)
22. F. Langa, P. Cruz, E. Espildora, A. Hoz, J. L. Bourdelande, L. Sánchez, and N. Martín, [*J. Org. Chem.*, 2001, **66**, 5033.](#)
23. A. A. Peyghan, H. Soleymanabadi, and M. Moradi, [*J. Phys. Chem. Solids*, 2013, **74**, 1594.](#)